

Three-dimensional, Broadband Seismometer Array Experiment at the Homestake Mine

V. Mandic, V.C. Tsai, G. Pavlis, T. Prestegard, J. Atterholt, D.C. Bowden, P. Meyers, R. Caton, [Boise? L. Liberty, Z. Li, G. Gribler]...

^a California Institute of Technology

^b Indiana University

^c School of Physics and Astronomy, University of Minnesota, Minneapolis, MN 55455, USA

Introduction

Seismology has been a ubiquitous tool for determining subsurface Earth structure and learning about various dynamic sources, including earthquakes and nuclear explosions [standard seismology REF]. The number of seismic arrays has grown appreciably in the last few decades, with over 7000 broadband seismometers deployed within the United States alone, and over 20,000 worldwide [iris REF]. However, despite this large number of seismometers, instruments have largely been confined to the Earth's surface, with few stations having been placed at depths greater than 100 meters, primarily due to the obvious practical difficulty of getting to such depths. The few exceptions include seismometer arrays within single boreholes (TCDP, Parkfield REF) and in active mines (S. Africa and other REF), and frequently such instruments have been limited to high-frequency geophones rather than more broadband seismometers [REF].

While observing ground motions at or near the Earth's surface has generally been acceptable, there are a number of reasons why observations at deeper depths, particularly from an array of instruments, would potentially be useful. First and foremost, it is well known that most seismic 'noise' is generated near the surface [noise REF] and that this noise generally decreases significantly with depth [borehole REF]. Observations at depth therefore have the potential to be less contaminated by surficial noise, and therefore may more accurately measure the elastic waves arriving from geophysical sources of interest. The second main reason that seismic measurements at depth could be advantageous is that Earth structure generally decreases in complexity with depth, with most of the highly weathered and sedimentary deposits being confined near the surface [REF]. Not only do such features typically cause much slower velocities, but they cause the Earth to be highly heterogeneous and strongly scattering, resulting in complexity of wave propagation that is challenging to model and interpret. Since nearly all observations contain this complexity, it is not known precisely how severe the effect is, but it is expected that observations far away from such heterogeneities to be simpler and more predictable.

For the above reasons, certain equipment that is very sensitive to ground motions have been proposed to be placed at depth, including the next generation of the Laser Interferometer Gravitation-wave Observatory (LIGO). Although LIGO has recently

successfully detected gravitational waves [Abbott REF], fully exploring the scientific potential of gravitational-wave observations requires more sensitive gravitational detectors that are currently partially limited by seismic noise, which causes small fluctuations in the local gravitational field in addition to the direct motion of the detector mirrors. Understanding and reducing this seismic noise is critical to future gravitational-wave detectors, and going underground may provide the solution.

To explore the promise that subsurface seismological observations have, both for geophysical and gravitational-wave applications, we have built and operated an underground three-dimensional (3D) array at the Homestake Mine in Lead, SD, which was one of the largest and deepest gold mines in North America; we report on this unique 3D array in this publication. The Homestake Mine officially closed operations in 2002, but reopened in 2007 as the Sanford Underground Research Facility (SURF), and currently features several other experiments, including dark matter and neutrino experiments that benefit from the cosmic ray shielding of the rock overburden. Due to the significant infrastructure in the Homestake Mine, including easy access to numerous underground levels with hundreds of km of available drifts, availability of power and network, and safety protocols make the Homestake Mine an ideal location for the development of a 3D seismometer array.

In this paper, we describe the novelty of the 3D Homestake array as compared to other subsurface seismological deployments, the experience learned in operating the underground array for 2 years, and preliminary results that demonstrate the potential that such data have. While the results described here are not expected to be the final products of the Homestake array, we anticipate the results to be useful both for future experiments of a similar type and as a foundation for later analysis.

Some topics not necessarily addressed in the introduction:

- Review of literature on applied geophysics underground measurements – this is a simple search in Geophysics. A LOT has been done for the mining industry and we need a perspective
- Basic geology review – note the rocks are schists and phyllites and high precision mapping data is preserved at Sanford lab
- Emphasize how the Homestake array is different from what was done in the past, enabling unique new studies (specify)

Seismometer Array

The Homestake seismometer array consisted of 24 seismic stations, 15 underground and 9 on the surface. The underground stations were scattered across several levels: one at the depth of 91 m, one at 244 m, one at 518 m, five at 610 m, three at 1250 m, and four at 1478 m. The locations of these stations were chosen to maximize the horizontal aperture of the array within the constraints imposed by safe access, availability of power, and access to SURF's fiber optic network. In several cases we had to extend existing power and network cables to support the stations. We strove to locate sites as far from activity in the mine and from water drainage pathways as possible. Stations were usually placed in alcoves or blind alleys to minimize the effects of the air drifts, although several stations were installed in enlarged areas in the main drifts of the mine. In

most cases, we found there were complex tradeoffs between cost of installation and distance from active operations.

Many sites had existing concrete pads of various sizes and thickness from the original mine operation. When necessary we poured a concrete pad was poured directly onto the rock. IN all cases a granite tile was attached to the pad using thinset mortar. All underground site preparation was completed by three months prior to the installation of the instruments. Each seismometer was placed directly onto the granite tile, and was oriented to cardinal directions using an Octans gyrocompass from the IRIS-PASSCAL instrument center. To reduce acoustic noise noise induced by air flow we covered each sensor with two nested huts constructed of 2" thick polyisocyanurate foam panels and sealed with foam sealant. The digitizer was placed several meters away, and included a Q330 data logger, a baler, and network and power supply electronics. Each station was powered by a small 12V battery continuously charged by a simple AC charger. The battery provided approximately a one day pwer reserve, which proved more than adequate to cover any power outages encountered during the experiment.. .

In addition to saving the data locally with a baler, we utilized real-time telemetry for all underground sites and six of the nine surface sites. The underground stations were synchronized using a custom-designed GPS optical distribution system. The GPS signal was received by a GPS antenna mounted on the roof of the SURF administration building and piped to a Q330 in the server room of the same building. This "master" Q330 data-logger was used to convert the received high-frequency GPS signal into the separate 1PPS (1 pulse-per-second) and NMEA metadata components that was used as an external timing signal for the underground instruments. The output from the master Q330's EXT GPS port was fed into an electro-optical transceiver to convert the analog voltage output to optical signals. The transceivers was custom-made for this application by Liteway, Inc. (model number GPSX-1001). An optical-fiber network of optical splitters and transceivers was installed underground to distribute this GPS timing signal to all underground stations, while maintaining its signal-to-noise ratio throughout the mine. At each station, a transceiver was used to convert the optical signals back into to electrical, which were then sent into the Q330's EXT GPS port. Phase errors logged by the Q330 suggest the timing precision achieved with this system was of the order of 1 μ s. [DO WE NEED MORE INFORMATION ON THIS? MAYBE A DIAGRAM?] Systematic errors from propagation and electronic delays are negligible.

Five of the nine surface stations were located on SURF property above the underground stations. One was located at Lead High School in collaboration with the Lead Deadwood Public School District. We deployed three stations on private land in an outer ring at a nominal radius of 5 km from the array center. We used conventional, portable broadband sensor vaults but with attention to an important detail commonly ignored in recent years. That is, we were careful to separate the wall of the sensor vault from the concrete pad poured at the bottom. This detail is known from early experience in the 1990s at IRIS-PASSCAL to reduce tilt noise from soil motions. All but one of the sites (DEAD) were bedrock sites with a concrete pad poured on weathered metamorphic rocks of variable lithologies. The surface stations were all oriented by conventional compass methods, which means the precision is less than the underground sites oriented with the Octans instrument. We insulated the sensor vault with a layer of foam and burial with as much of a soil cover as possible. We had the common problem of rain washing some cover way that we restored when the instruments were serviced. The six inner stations all used radio telemetry. The sites on SURF property and the site RRDG were linked by a master radio at on the roof of the Yates administration building where our data logging computer was located. The Lead High School (LHS) site used a point-to-point radio that linked the outdoor site to a Linux computer in a computer laboratory at the school. All surface sites except LHS used solar power. LHS used an

AC system similar to underground sites but with a larger battery backup. All surface sites used the standard Q330 GPS timing system.

The telemetry system we deployed used a computer running the Antelope software at the Yates Administration building to handle real time communication to all underground sites and five of the nine surface sites. We ran a separate Linux computer running Antelope at LHS to handle real time communications with that single site. This approach was necessary to deal with firewall issues at both SURF and the high school. In both cases it was easier to get permission to override blocking of a nonstandard port to a single host than a long list of ip numbers for the array instrumentation. We then set up an orb2orb feed to a University of Minnesota computer that acted as a data concentrator. The participating institutions and the IRIS-DMC were then able to tap that connection for real-time feeds with a latency of a few 10s of s. Minnesota developed a custom monitoring system to test for our of range conditions and build a web-based quality control quick look system. We set up a rotating shift schedule to monitor the diagnostic information on daily basis. This allowed us to quickly identify and diagnose problems. This was a major factor in the exceptionally high data recovery rate of this experiment (near 100% for every site except DEAD, which had power problems in the winter of 2015-2016). Furthermore, the telemetry data have no mass position related issues except for two sensors failures. In addition, this quality control monitoring allowed us to detect and diagnose a subtle problem on station E2000. That station began showing odd tilt transients, which site visits revealed was created by failure of the thinset grout on the base of one of our granite tiles. This was repaired by pouring a new concrete pad and setting the tile directly in the concrete.

All of the underground stations were installed between December 2014 and March 2015, and remained operational until December 2016. The surface stations were installed in May 2015 and remained operational until September 2016. The seismic equipment used in the experiment was provided by the Portable Array Seismic Studies of the Continental Lithosphere (PASSCAL) instrument center, which is part of the Incorporated Research Institutions for Seismology (IRIS). Most stations used a Streckheisen STS-2 high-sensitivity broadband seismometer. The exceptions were the underground station 300 and three surface stations where we deployed more water resistant Guralp CMG-3T seismometers.

Figure 1 shows the map of the Homestake array stations. The locations of stations are known with uncertainties on the order of 2 m. Underground station locations were obtained from maps of the mine drifts based on past mine surveys, while surface station coordinates come from GPS data.

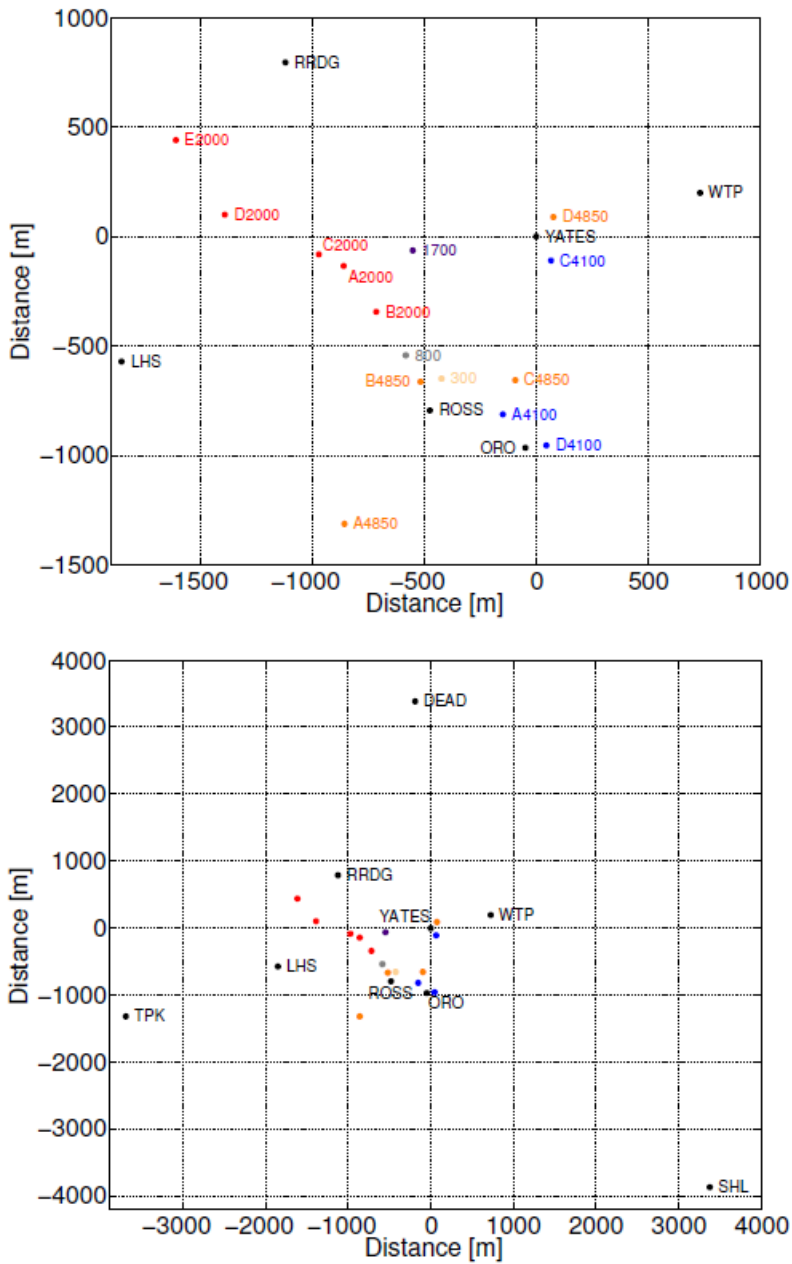


Figure 1: [PLACEHOLDER] Homestake array layout, relative to Yates shaft station (at origin). A zoomed-in view with the underground stations labeled is shown on top (DEAD, SHL, and TPK not pictured). All stations are shown in the lower plot, but only the surface stations are labeled.

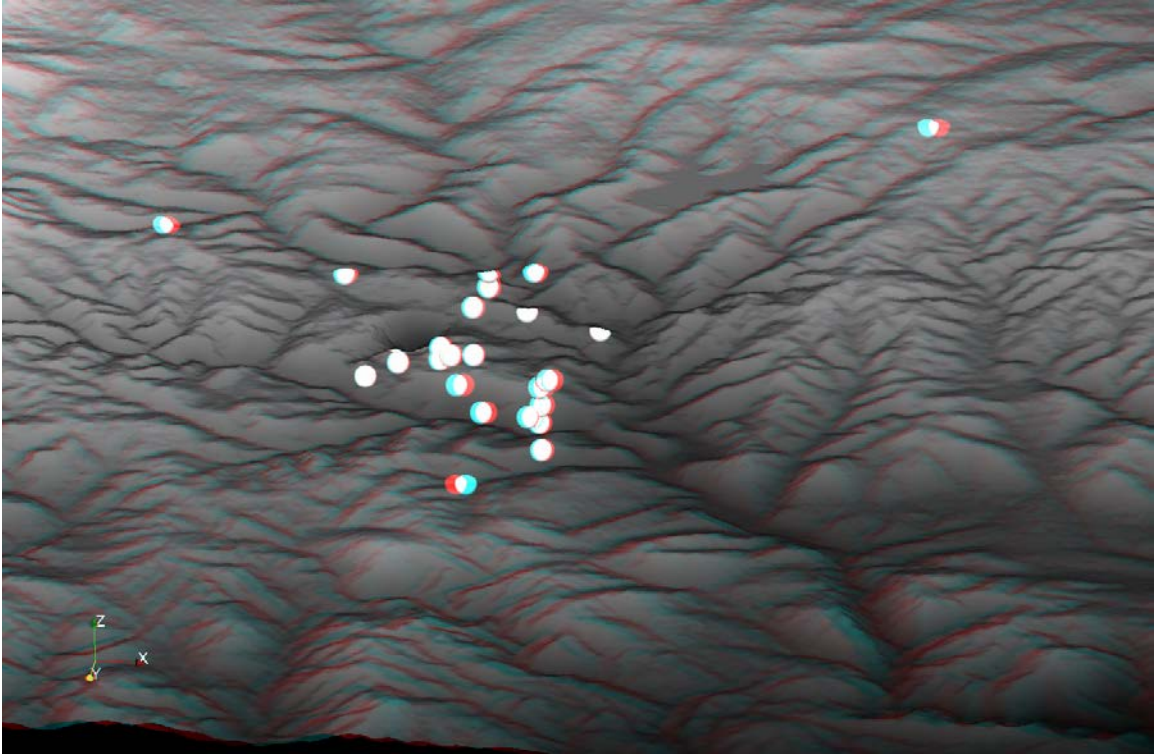


Figure 1. Possible alternative style figures for array geometry

Active Experiments (Gary, with help from Victor, Boise)

- Surface Land streamer data
 - Surface recording with land streamer
 - Recorded in underground by passive array stations
 - Timing failure lead to need to estimate origin times independently (That will better be left to a different paper.)
 - Might show a record section of some of that data
 - Need a map figure of shot geometry
 - Problem – mismatch of bandwidth of broadband and this source. Would have had better results with auxiliary geophones and/or a source that had more output at lower frequencies.
- Underground HSP experiments
 - 3 locations
 - sensor emplacement and anchoring
 - sensor orientation method
 - 9 component shooting
 - walkaway geometries
 - Need a number of maps to document this geometry.
- Underground land streamer experiment
- Critical review of approaches we used

- Streamer collected a lot of useful data fast, but sleds were problematic in this location. Something more like a real streamer would probably have been more workable
- Airless jackhammer was effective, but produced a very high frequency pulse when applied to bare rock. Also produced a huge airwave. Stronger source would have been helpful but there are strong safety tradeoffs. Pulse was so high frequency was nearly invisible on broadbands when only a few m away. (actually we need to look more closely at that) I know we can see spikes on the near station, but could not see it elsewhere – should confirm that.
- Geophone coupling a huge unknown that may contaminate our data. (details later). A more effective strategy would have been to do what SDSMT people did – use a rock drill and anchor sensors to the wall with a rock bolt. Note that is the opposite approach where you aim to collect tons of data fast and beat down noise by averaging.
- Water everywhere and always complicating things.

Preliminary Results

Noise Spectra

This needs an introductory, motivational paragraph. Consider having Ross show a figure he has showing the SNR of the tidal component on horizontal components to make the point that these data are super quiet at ultra long periods.

We compute the amplitude spectral density (ASD) of seismic noise over long periods, for different stations and different seismic channels (east, north, vertical). These are shown in Figure 2 in comparison to the low- and high-noise models by Peterson [REF]. We use one year of data (from June 1, 2015–May 31, 2016), split into 400 second intervals. For four of the surface stations, we use only 3 months of data (the rest is not yet available).

All spectra show the median amplitudes in each frequency bin for the vertical seismic channel.

The top-left panel compares the ASDs for stations at several different depths. All of the stations are in close agreement in the middle range of frequencies, which corresponds to the microseismic peak. At higher frequencies, there is significantly less noise with depth: above 0.5 Hz, the stations at 4100 ft and 4850 ft depths are nearly an order of magnitude quieter than other stations. At the lowest frequencies there is also a good agreement between the stations, although a slight trend of decreasing noise with depth is apparent; this may be due to larger temperature variations closer to the surface inducing tilts in the concrete pads.

For the surface stations (top-right panel) there is a wide range of variability; this is due to differences in the local environment in terms of thermal insulation and proximity to human activity. Differences in the microseismic peak (0.1–0.2 Hz) are likely due to differences in the amount of data used in this analysis; the microseism experiences seasonal variations and appears differently for stations which do not include the full year of data (DEAD, SHL, TPK, and YATES).

The middle-left panel shows spectra for stations at 300 ft, 800 ft, and 1700 ft depth. The noise levels are reduced with depth at higher and lower frequencies; the higher level of low frequency noise at the 800 station is likely due to its proximity to one of the mine shafts. The middle-right

panel shows spectra for the stations at 2000 ft depth. There is generally good agreement between the stations across all frequencies. B2000 experiences increased noise, especially at high frequencies, likely due to its location near a lunch room and a mine shaft.

Spectra for the stations at 4100 ft depth are shown in the bottom-left panel. The C4100 station appears to have the least noise at low frequencies, while the D4100 station experiences the most high-frequency noise. These variations are not well-understood based on station locations and expected proximity to human activity. Finally, spectra for the stations at 4850 ft depth are shown in the bottom-right panel. Here, the B4850 station experiences significantly increased high-frequency noise due to its location near a large fan and ongoing construction. Above 1 Hz, the other stations are in fairly good agreement, although each station seems to have its own individual noise peaks in the spectrum. This is likely due to the unique environment surrounding each station:

C4850 is in a storage room and very close to a rail line, and D4850 is very close to other experiments in the mina, ventilation equipment, and human activity. The A4850 station seems to have more overall high-frequency noise than these two stations, which is not well-understood since it is one of the most isolated stations in the entire array.

Figure 3 shows ASD histograms for the RRDG surface station (left column) and for the A4850 underground station (right column) as examples of a relatively good surface station and our deepest and most isolated underground station. Here, we show histograms of ASDs calculated from the 400-second data intervals over 1 year in each frequency bin, revealing the overall variability of the seismic noise at each station. The white curve represents the median ASD (identical to those shown in Figure 2), the black curves represent the 95% confidence intervals in each frequency bin, and the color scale shows the overall distribution. The Peterson low- and high-noise models are shown in dashed gray.

The histograms display about two orders of magnitude of variation across all frequencies for both the RRDG station and the A4850 station. The A4850 station measures less noise in general and appears to have less overall variation than RRDG. There also appears to be significantly more high-frequency noise in the RRDG station; this is likely due to anthropogenic surface waves that are suppressed with depth. Both stations stay within the low- and high-noise Peterson models most of the time; in the 0.3–0.9 Hz range, the A4850 station is actually below the low-noise model a significant fraction of the time. There is also a considerable difference between the vertical channel and the horizontal channels at low frequencies: at 0.01 Hz and below for both stations, the vertical channel has almost an order of magnitude lower noise than the horizontals.

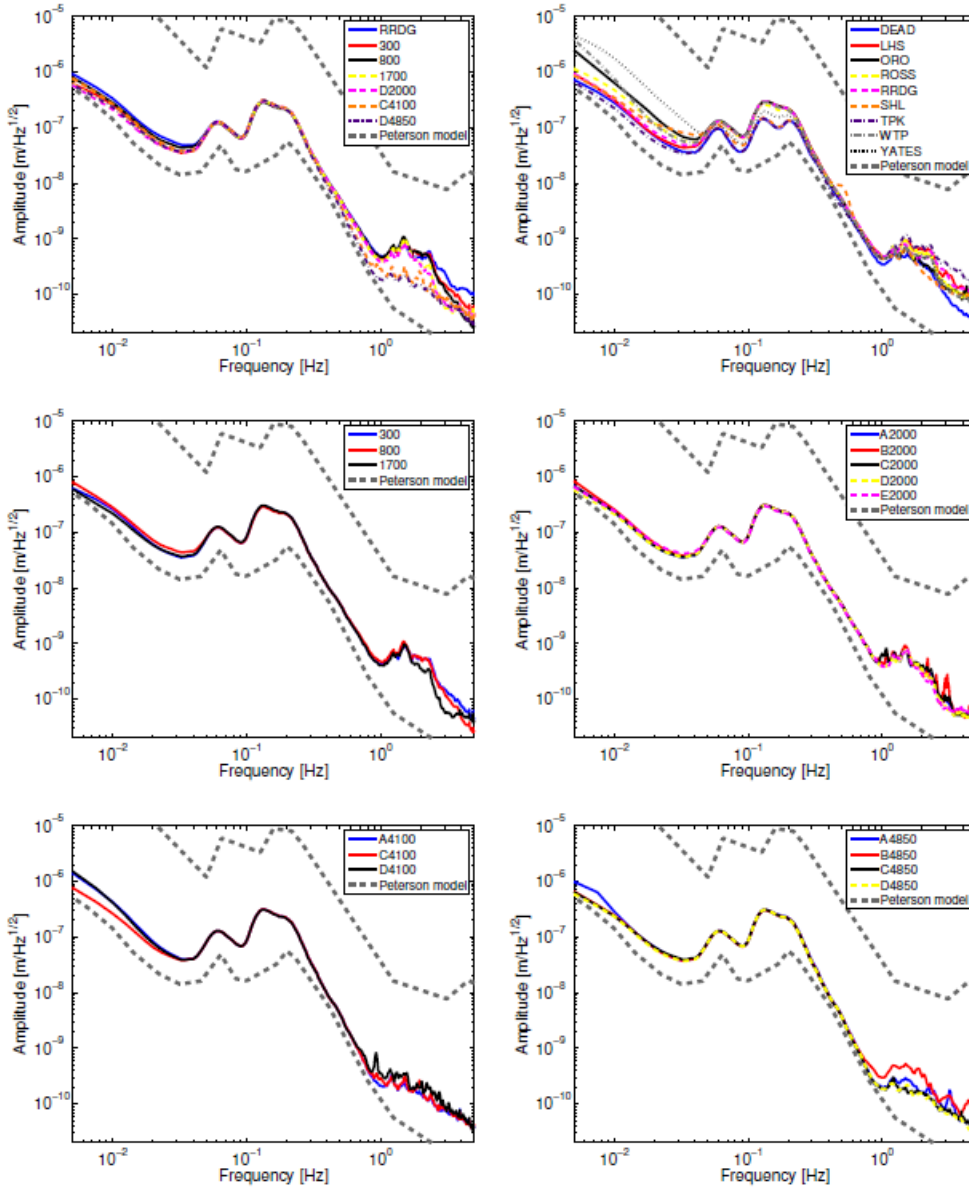


Figure 2: [PLACEHOLDER] Median amplitude spectral densities for all Homestake stations; numbers in the legend entries denote depth in feet, while numberless legend entries denote surface stations. One year of data is used except for DEAD, SHL, and TPK stations, for which only 3 months of data was used, and YATES, which is missing data due to power and communication issues. More details are provided in the text.

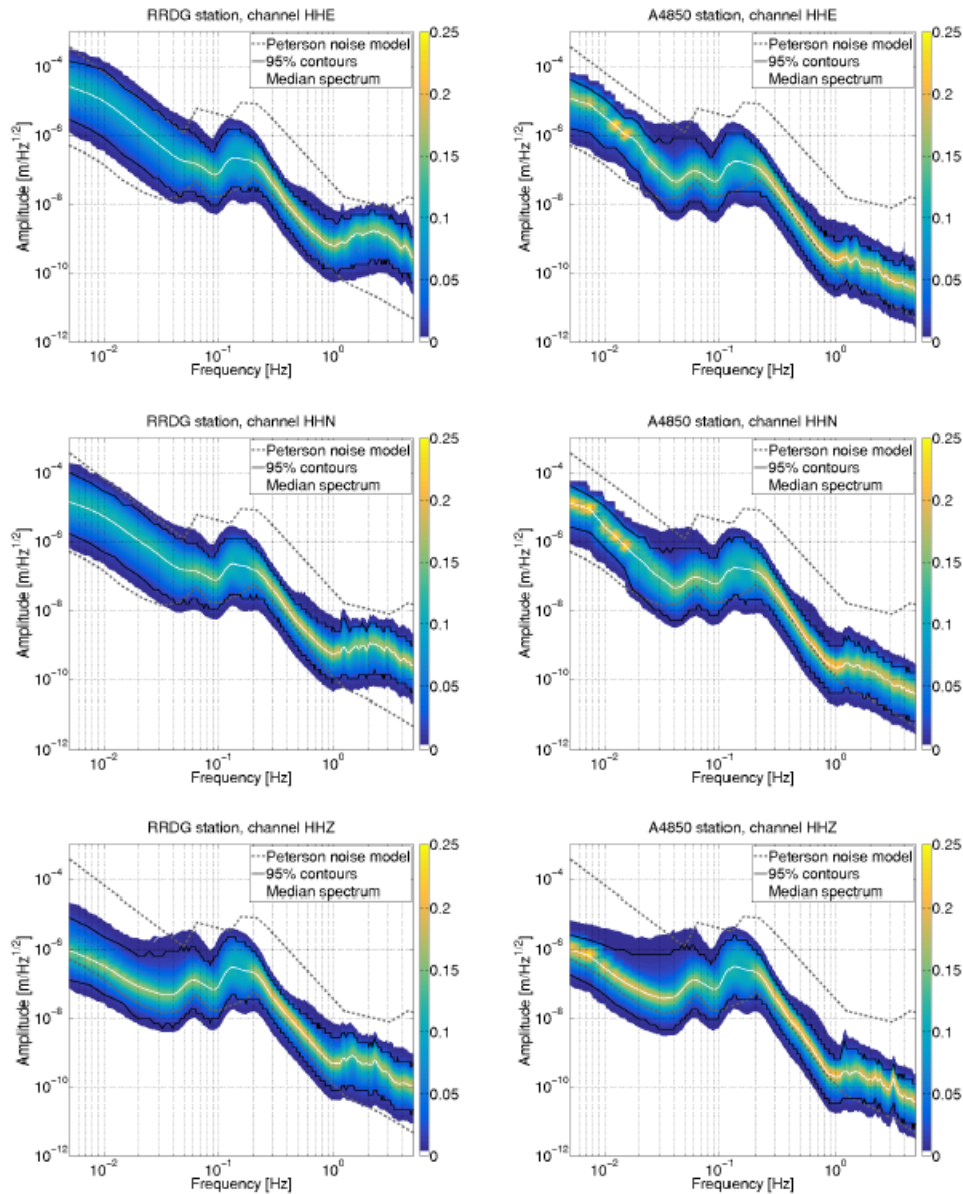


Figure 3: [PLACEHOLDER] Histograms of amplitude spectral density in each frequency bin for a surface station (left column) and for an underground station at 4850 ft depth (right column). The plots are divided into rows by channel: east (top), north (middle), and vertical (bottom). Median ASDs (solid white), 95% confidence intervals for each frequency bin (solid black), and the Peterson low- and high-noise models (dashed gray) are shown. See the text for more details.

Array Analysis of Event Data

To date we have processed six months of data to identify seismic events. This has required a mix of conventional and unconventional analysis. A technical problem we faced is that this array was located in an area with some of the sparsest coverage in the country (Figure EVENTMAP – needs to include regionals stations). In an area with sparse coverage, an array of 24 ultra quiet sites dominates detection limits and violates implicit assumptions of conventional automated detectors. Figure EVENTMAP shows

the 8 regional stations we used to detect and locate local and regional events. We used the automated detectors and location system in the Antelope 5.6 (<http://brtt.com> latest access April 25, 2017). When we used all channels from the array in combination with the sparse regional coverage we had a large number of spurious detections. Although some are definitely local sources and might be of interest in other studies, our initial interest was the events with the best signal-to-noise ratio where the plane wave approximation was valid for phased array processing. We reduced the false detection rate to near zero by running the detection algorithm only on the three outer surface sites (DEAD, TPK, and SHL) and one of the quietest underground sites (D4850) and required six P-wave associations before declaring an event. The most significant impact on this choice is that with this scheme we dropped all of the events from the local mine with example seismograms shown in Figure LOCALMINE. The source for those seismograms is without doubt an active surface mine whose boundary is only 2.5 km west of station TPK. Figure EVENTMAP is thus incomplete, as it does not show any events from this potentially useful data source. Review of data from initial detector runs that detected these events indicate this mine blasts at least once per day during the workweek. There are thus a large number of seismograms like Figure LOCALMINE that could be used in future studies.

We used a standard analyst review method to produce the epicenter maps shown in Figure EVENTMAP. That figure shows 431 epicenters, of which 359 are in the local area shown in b and 72 are at regional to teleseismic distances. The locations of the distant events are plotted in Figure EVENTMAPa. The locations shown were produced by association with epicenter estimates produced by U.S. Geological Survey catalogs and assembled at the USArray Array Network Facility (<http://anf.ucsd.edu/events/> last access April 27, 2017). We estimated the local event epicenters shown in Figure EVENTMAPb with the dbgenloc program (REFERENCE) using the IASP91 earth model using travel time picks made by standard, interactive analyst review methods. Every one of 359 events shown in Figure EVENTMAPb are almost certainly mining explosions from coal mining in the Powder River Basin. All have similar waveforms with emergent P waves and prominent surface waves like the event shown in Figure BLAST. We assumed that was the case and fixed the depth of all these events for the location estimates used for Figure EVENTMAPb. Most of the events cluster in the area of the coal mining district. There are some outliers that are almost certainly poorly constrained epicenter estimates that have been badly mislocated. These events are characterized by picks at only one regional station in addition to the array, which creates a poor constellation for location. This problem is solvable by using an array slowness vector estimate by plane wave processing like that described below, but at the time of submission we had not completed that processing. Most, if not all, of the scattered epicenters in Figure EVENTMAPb are likely explosions from Powder River Basin coal mines.

Figure LOCALBLAST shows a first order observation from this array. As expected theoretically the Rayleigh wave from this explosion decreases systematically with depth. With the true amplitude scaling of Figure LOCALBLAST the Rayleigh is barely visible on any of the stations in the 4000s subarray.

We processed all the events with locations shown in Figure EVENTMAP with a nonstandard array processing method. When we examined waveforms recorded by the array it was immediately clear that simple delay and sum phased array processing was problematic. Notice that the broadband P waveforms seen in Figure TELEa-b are very well matched for this large event for only the first cycle of the P wave. When the same data are filtered to short periods (Figure TELEd) there are very large variations in the waveforms at distance scales that are a fraction of the wavelength of P or S body waves. Although not shown surface and underground waveforms in the short period band are commonly wildly different. Figure BLAST shows this problem is even more dramatic for typical coal mine explosions from Wyoming (Figure EVENTMAPb). Note the very strong changes in amplitude and waveform shape for subarray stacks from different levels in mine.

Because of the depth dependence of waveforms we processed these data using a program called dbxcor (Pavlis et al., 20??) in a subarray mode. That is, we grouped the array stations with the grouping shown in Figure LOCALBLAST. We processed each of the 3 subarrays independently with dbxcor. dbxcor was originally designed for large aperture arrays like the USArray but we found it worked well in this setting. dbxcor does not use a plane wave approximation, but computes lags relative to a stack estimated by a robust method described by Pavlis et al. (201??). Figures TELEa-c and BLASTa-b show the three-components of the stack of the aligned seismograms from each subarray. Figures TELEd and BLASTc show typical aligned seismograms that were used to construct the stack seismogram. Note, however, that in dbxcor processing the cross-correlation window was always much shorter than shown in these figures and defined interactively by the analyst. Typical correlation window sizes were 2-4 s for the local mining blasts and 10-20 s for teleseismic events. We have found no unbiased way to correlate subarray stacks to more precisely measure time delays between subarrays. Consequently, at present we have only used manual picking to align subarrays as shown in these figures.

Not sure where or what interpretations we should make here. If coauthors think it worth developing for this particular paper, I think I can at least write an essay to argue:

1. There is a suggestion of P to surface wave scattering in the teleseismic event. The argument is that for the nominal period of 1 s for these data, the wavelength for P is 6 km and S is 3.5 km. We are seeing large variations in waveforms over distances of the order of 200-300m which I find hard to explain with some type of scattering. Not sure we can convincingly say surface waves modes are required though? topic for discussion at our next call
2. I think there is clear evidence for a depth dependence in amplitudes for the mining explosions.
3. A harder thing to argue I think these data hint at is strong scattering of the Pg phase we observing in the crust between the source and this array. All forms of crustal scattering will add interfering signals that get more and more prevalent with lag time from the first arrival because more and more single and multiple scatterers become feasible.

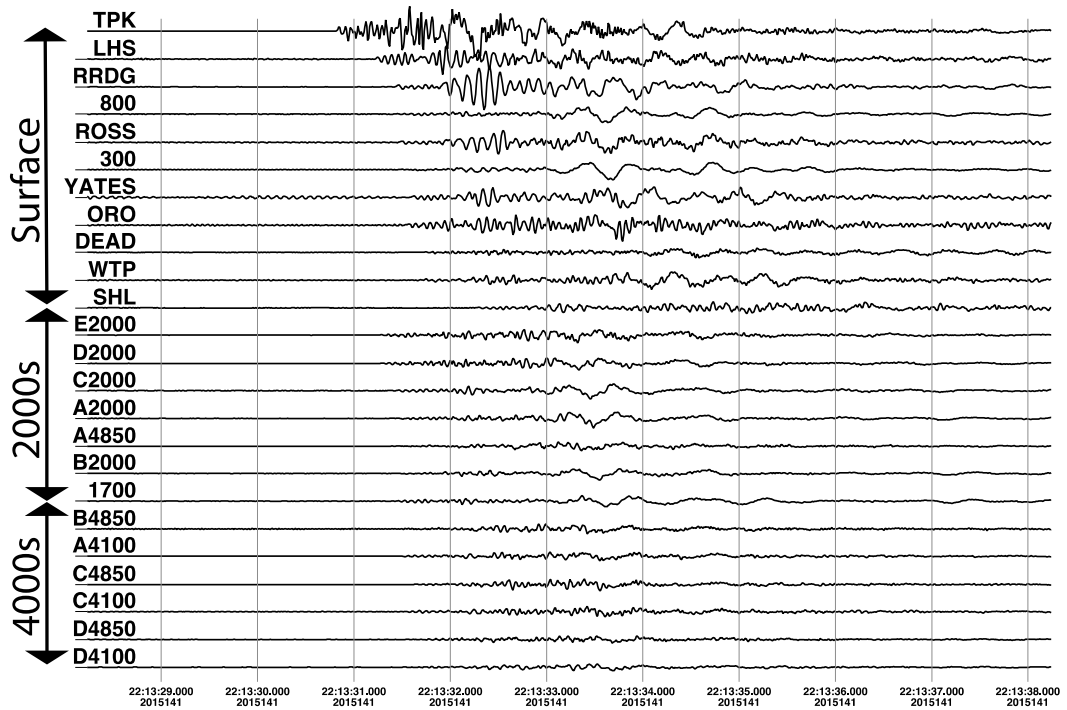


Figure LOCALBLAST. Vertical component seismograms from local surface mine. Seismograms are displayed at true amplitude and grouped by subarrays used throughout this paper. Records for each subarray are sorted by epicentral distance from the estimated source location (approximately 4 km west of TPK). Subarrays are ordered by increasing depth.

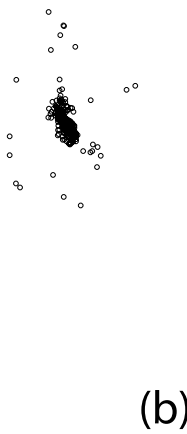
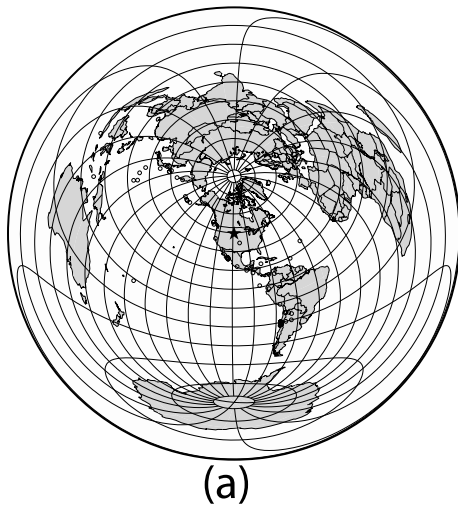


Figure EVENTMAP. Epicenter maps of events recorded by Homestake 3D array. (a) is an azimuthal equal distance projection map centered at the array site marked with a star. Epicenters of distant earthquakes recorded the array in the 2015 study period are shown as circles. (b) is comparable but focused on local and regional events. The array location is again shown as a star and estimated event epicenters are shown as circles. Black filled triangles are regional stations used for detection and location of the events plotted.

Figure TELE. Alaska earthquake records from Homestake 3D array. (a) illustrates the three components of subarray stacks defined in the text. (a) shows the first 2 minutes of the data following the P wave signal. These data were filtered with 0.01 to 2 Hz bandpass filter before stacking. The P wave of this event is much smaller than the pP phase seen approximately 25 s after P (event depth is 120 km and distance is 33°). (b) shows a shorter time window focused on only the P wave (6 s following measured P time). (c) shows the vertical component seismograms stacked from the 4000s subarray that were stacked to produce that component in (b). (d) is identical to (c) except each seismogram was filtered with a short period filter (0.8 to 3 Hz 5 pole butterworth bandpass filter) to illustrate that the primary signal variation is at the highest recorded frequencies. All plots are true amplitude meaning amplitudes differences between seismograms are real. In all figures the seismograms have been aligned by cross correlation before stacking. Stacks are aligned manually.

Figure BLAST. Seismograms from a typical Powder River Basin coal mining explosion recorded by the Homestake 3D array. All the data shown in this figure were filtered with a 5 pole Butterworth filter with a pass band from 0.25 to 10 Hz. (a) shows 2 minutes of data following P and is directly comparable to Figure TELEa. (b) and (c) are directly comparable to Figure TELEb and c respectively but for this explosion source instead of a teleseismic earthquake. (b) shows subarray stacks for 6 s of data following the measured P wave time. (c) shows vertical component component seismograms stacked to produce the 2000s subarray, vertical stack in (b). We show the 2000s subarray here because for this event that subarray is oriented roughly in the direction the P wave is propagating. All figures show seismograms in true amplitude as in Figure TELE and seismograms were again aligned by a mix of cross-correlation and manual picks.

Conclusions (TBD, let's see what the paper looks like)

- Useful data with a wide range of scientific use to better understand wave propagation
- Emphasize low noise, high SNR potential – especially at very long periods
- Preliminary indications about velocity distribution etc
- S-wave speed estimates from underground land streamer (3.5 something + or – something) with small differences in the different named formations.

